Reservoir uncertainty description via petrophysical inversion of seismic data

Miguel Bosch[1], Gustavo Bertorelli[2], Gabriel Álvarez[2], Adriana Moreno[3], and Raul Colmenares[3]

Abstract

Hydrocarbon reservoir characterization commonly combines seismic, petrophysical, and well-log information in a variety of procedures. As an inference problem, this combination can be formulated in a unified inverse framework, reducing the bias of nonlinear relationships among intermediate variables and providing a comprehensive calculation of uncertainties at final estimates of the medium parameters. In addition, the unified formulation leads to the joint estimation of reservoir and medium elastic properties as well as related parameters of interests. This problem is formulated from a set of continuous variables that commonly characterizes the reservoir (total porosity, shale volume fraction, and water saturation), which can be related to the medium mechanical properties with a petrophysical model calibrated to the specific setting of the reservoir and target stratum. The joint model property configuration is related to the observed seismic data via Zoeppritz incidence-angle-dependent reflectivity and convolution with a source wavelet for each CDP gather. Data and calibrated information are combined in a posterior probability density of the model parameters that is evaluated with a sampling approach, using a Markov-chain Monte Carlo algorithm. From a large number of realizations, one can calculate expected values and full marginal probability distributions for reservoir properties and elastic properties. The method is illustrated with the estimation of reservoir parameters at a gas reservoir presenting a Class 2 AVA response, with focus on the estimation of water saturation. The calculated saturation probability distributions show coherent results with the known saturation at various well locations.

Introduction

Measurement of reservoir properties such as hydrocarbon saturation, porosity, or shale volume fraction commonly is based on well logs, which are characterized by short penetration away from the borehole. The vertical resolution of these data is particularly fine, but lateral sampling of the reservoir area is scarce and cannot provide a 3D description of the reservoir on its own. On the other hand, 3D seismic surveys provide information with a full spatial coverage of the reservoir up to a scale limited by the seismic wavelengths. Seismic-reflection amplitudes, times, and phases carry information on the elastic-medium parameters, which are related to the reservoir properties via petrophysical or statistical relationships. Thus, several methods that combine seismic and rock physics are used for the inverse estimation of seismically derived reservoir properties with 3D coverage of the reservoir. Bosch et al. (2010) give a review of this.

An important issue to address in these methods that combine rock-physics models with seismic data is the uncertainty on the estimated reservoir properties. The uncertainty is related to acquisition of the seismic and well-log data, data processing, physical and numerical modeling of the data, the selected rock-physics model, its calibration against well-log information, and its deviation statistics (see Grana et al. [2012] for a description of rock-physics models and uncertainty). In addition, another source of uncertainty is associated with the capability of the composed rock-physics and seismic models to decouple different parameter variations from the seismic signal in a specific reservoir setting. Poor property resolution might result from weak sensitivity of the seismic signal to a particular reservoir-property variation.

A common example is the small seismic sensitivity to fluid (water-oil) substitution in some heavy-oil reservoirs because of density similarities between water and oil. More often, poor property resolution is related to similar seismic effects produced by the variation of different reservoir properties and whether those differences are beyond the data uncertainties. Common examples are large reflectivities (bright spots), which in some cases might be caused by fluid, porosity, or lithology changes. Thus, the uncertainty associated with the reservoir properties estimated by combining seismic and rock-physics models is variable, highly dependent on the conditions of the reservoir formation and the available data, and requires to be described.

A general description of the reservoir-property uncertainty is given by the joint posterior probability density function (PDF) of the reservoir parameters and its marginals or by the cumulative probability distribution function (CDF). We estimate these PDFs to provide a full description of the posterior uncertainties in the setting of a producing gas field. The target stratum is a gas-bearing clean sand sealed by a shale stratum and close to an underlying crystalline basement.

In the joint rock-physics and seismic inversion we apply in this work, the posterior PDFs combine the uncertainties associated with the seismic and rock-physics components of the model as well as with the seismic data and prior information from well logs. Because this is a siliciclastic environment, we parameterize the reservoir description in total porosity, shale fraction, and water saturation. Only two fluids are present, and hence gas saturation is the complement of water saturation. We focus our estimation effort on quantifying the saturation, not only on providing a gas indication. The reservoir medium is considered elastic and isotropic and is parameterized by the seismic P-wave velocity, S-wave velocity, and mass density.

Joint petrophysical and seismic posterior PDF

The scheme of Figure 1 presents the information and relationships that we model to solve the combined rock-physics and seismic inverse problem. The figure shows the parameter components (subsets) that we include in the model. These parameters are considered random and are associated with corresponding probability density functions. They are grouped in

[1]Universidad Central de Venezuela.
[2]Pacific Rubiales Energy.
[3]Info Geosciences Technology and Services.
http://dx.doi.org/10.1190/tle34091018.1.

1) reservoir parameters, $\mathbf{m}_{res}$, which correspond, as previously mentioned, to total porosity, shale fraction, and water saturation, defined over a regular spatial grid in horizontal position and seismic-reflection TWT
2) elastic parameters, $\mathbf{m}_{elas}$, corresponding to V_P, V_S, and mass density defined over the same grid
3) rock-physics model parameters, $\mathbf{m}_{rmod}$, which are a set of parameters that governs the rock-physics model (such as critical porosities, water and gas density, and compressibility)
4) seismic-source wavelet deviations from the prior wavelet, $\mathbf{m}_{source}$
5) data, $\mathbf{d}_{seis}$, that correspond to the prestack seismic gathers in a time window that encompasses the reservoir, transformed from offset to incidence-angle domain

Figure 1 depicts the direct acyclic graph that relates the model components and data, with indications of the random parameter components of the model, the data parameters, and their relations.

The posterior PDF on the joint model parameters corresponding to the graph in Figure 1 is composed as a product of (1) prior PDFs on the ancestor model components (i.e., model components that are not conditioned directly by other model components), (2) conditional PDFs for the descendent model components, and (3) a seismic-data likelihood function, which depends directly on the elastic and source model parameters,

$$\sigma(\mathbf{m}_{res}, \mathbf{m}_{rmod}, \mathbf{m}_{elas}, \mathbf{m}_{source}) = c\rho(\mathbf{m}_{res})\rho(\mathbf{m}_{source})\rho(\mathbf{m}_{rmod})\rho(\mathbf{m}_{elas} \mid \mathbf{m}_{res}, \mathbf{m}_{rmod}) L_{seis}(\mathbf{m}_{elas}, \mathbf{m}_{source}). \quad (1)$$

Above, $L_{seis}(\mathbf{m}_{elas}, \mathbf{m}_{source})$ is the seismic-data likelihood function that measures the calculated and observed fitness of the seismic gathers; $\rho(\mathbf{m}_{elas} \mid \mathbf{m}_{res}, \mathbf{m}_{rmod})$ is the conditional PDF of the elastic-medium parameters for the given parameters of the rock-physics model and reservoir properties; $\rho(\mathbf{m}_{res})$, $\rho(\mathbf{m}_{source})$, and $\rho(\mathbf{m}_{rmod})$ are prior PDFs of the reservoir properties, source wavelets, and rock-physics model parameters, correspondingly; and c is a normalization constant.

The definition of the priors, conditionals, and likelihoods on the right-hand side of equation 1, along with the graph plotted in Figure 1, conforms an inference network (also called Bayesian network or belief network). The network operates with seismic data to estimate the reservoir parameters and their CDFs without local conditioning to the properties measured by well logs.

Figure 2 shows the reduced inference networks for two additional problems addressed before the seismic inversion — one related to the calibration of the rock-physics model and the second related to the calibration of the source wavelet. The calibration networks operate with well-log data in the first case and with well-log data and seismic gathers at well locations in the second case. For the calibration of the rock-physics model (Figure 2a), the input data are the elastic-medium parameters (V_P, V_S, and mass density) estimated from well-log measurements of eight wells.

The shale fraction, total porosity, and water saturation calculated from the corresponding well-log data were available for most of these wells and were accounted for as prior information. Given the elastic and reservoir properties, the objective of the calibration network is the estimation of the parameters of

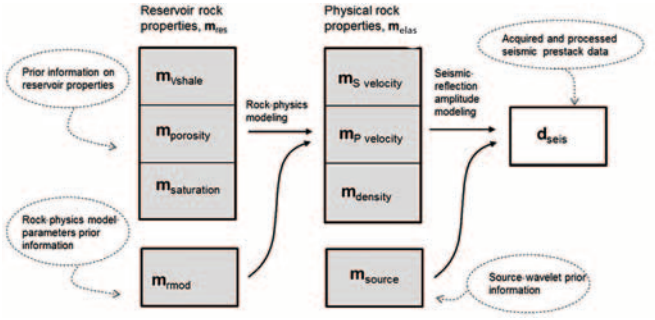

Figure 1. Inference network for inversion of seismic prestack data combining a reflectivity-convolutional seismic model and a rock-physics model. Bold arrows indicate direct dependencies across the random variables and their modeling direction. Variables in common blocks are modeled jointly. Gray boxes indicate model parameters, and white boxes indicate data that describe the seismic observations. Dashed ellipses and arrows describe the sources of prior information and data.

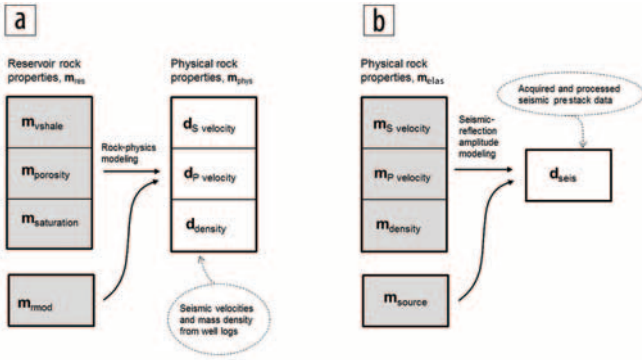

Figure 2. Inference networks for (a) calibration of the rock-physics model parameters using well-log data and (b) calibration of the source wavelet using prestack seismic and well-log data on seismic velocities and mass density.

the rock-physics model, $\mathbf{m}_{rmod}$. The joint posterior PDF for the model parameters is

$$\sigma(\mathbf{m}_{rmod}, \mathbf{m}_{res}) = c\rho(\mathbf{m}_{rmod})\rho(\mathbf{m}_{res})\, L_{well\ log}(\mathbf{m}_{res}, \mathbf{m}_{rmod}). \quad (2)$$

Here, $L_{well\ log}(\mathbf{m}_{res}, \mathbf{m}_{rmod})$ is the likelihood function that measures the fitness between the observed and calculated elastic parameters (V_P, V_S, and mass density) at well locations. The marginal probability of the rock-physics model parameters is obtained by integrating expression 2 with respect to the reservoir parameters to attain the posterior PDF of the rock-physics parameters, unconditioned by the elastic and reservoir configuration.

For the calibration of the source wavelet (Figure 2b), the input data are the seismic gathers at the well locations, and the prior information corresponds to the elastic parameters derived from well logs. The posterior PDF in this case is

$$\sigma(\mathbf{m}_{elas}, \mathbf{m}_{source}) = c\,\rho(\mathbf{m}_{source})\, L_{seis}(\mathbf{m}_{elas}, \mathbf{m}_{source}), \quad (3)$$

and the marginal PDF on the source deviations is obtained by integration of the above expression. From a formal point of view, the posterior expression of the rock-physics model parameters (equation 2) can be regarded as the limit case of equation 1 when the seismic-data uncertainty tends to infinity, and the posterior expression for the source-wavelet calibration (equation 3) is the

corresponding limit of equation 1 when the reservoir-property prior uncertainty tends to infinity.

Monte Carlo sampling

To generate solutions from the seismic and rock-physics inference network, two major approaches are (1) the search of a maximum posterior probability-model configuration (MAP) and (2) sampling the posterior PDF by drawing a large number of realizations. Because we aim for a full description of the uncertainties, we follow the sampling approach here, using Markov-chain Monte Carlo (MCMC) methods. The first approach commonly is limited to a search of a local mode.

In this area, conventional deterministic (MAP) elastic inversions and gas indicators were elaborated first. In continuation, the joint petrophysical and seismic stochastic-inversion method described here was applied at selected areas that encompass compartment prospects for uncertainty description.

The MCMC sampling method was adapted to the structure of the posterior PDF following the graph direction. First, prior realizations of the reservoir parameters are drawn from the corresponding prior PDFs. Second, a realization of elastic parameters is drawn from the conditional PDF. Third, the seismic gather is calculated from the elastic properties; we calculate the exact Zoeppritz reflectivities and convolve them with the source wavelet for this purpose. Finally, the realization is accepted or rejected according to the Metropolis rule, taking the ratio of the likelihood functions between the candidate and current realization.

The chain is repeated a large number of times, which warrants a convergence of the outcomes to a sample of the posterior PDF. Posterior estimates and frequency histograms are calculated from the sampled realization set. The inversion is performed CDP by CDP.

A similar procedure is used for the rock-model parameters and source-wavelet calibration chains. To model the source wavelets for all incidence angles in the gather, two source reference wavelets and their random deviations were parameterized at small and large incidence angles, being the intermediate incidence-angle wavelets interpolated from the two reference wavelets. The seismic and well-log data corresponded to the locations of the eight wells, which are taken into account simultaneously in the calibration. In all cases, the time range was limited to a window that included the target sand strata. Calibration of the rock-physics model and source wavelet is done before the seismic-inversion procedure so as to use the calibrated estimates of these two model components as prior information for the seismic inversion.

The rock-physics model

The rock-physics model that relates reservoir and elastic parameters includes a central transform and random deviates. The transform was based on common rock-physics methods for siliciclastic sequences. The dependency of the bulk and shear modulus of the rock matrix was modeled with the critical porosity model, as the inverse power of the difference between the total and critical porosity. Fluid incompressibility and matrix shear and bulk modulus for mixtures followed the Wood's model (weighted harmonic average), and the effect of fluid-filled pores was modeled by the Gassmann equation. The transform depends on a series of parameters, such as critical porosities,

incompressibility of gas and water, shear and bulk moduli of sand and shale with no pores, and densities of water, gas, sand, and shale.

We also introduced exponents to the inverse relation of the moduli with the porosity. A total of 21 rock-physics model parameters was required to define the central transform, $\mathbf{F}(\mathbf{m}_{res}, \mathbf{m}_{rmod})$, that estimates the P-wave velocity, S-wave velocity, and mass density from the total porosity, shale fraction, and water saturation,

$$\mathbf{m}_{elas} = \mathbf{F}(\mathbf{m}_{res}, \mathbf{m}_{rmod}) + \Delta\mathbf{m}_{elas}, \quad (4)$$

where $\Delta\mathbf{m}_{elas}$ are the deviations between the rock-physics model prediction and the actual true value of the elastic parameters. We characterize from the well-log data the statistics of these rock-physics model deviations to build up the conditional density of the elastic parameters. Assuming Gaussian deviations and characterizing the deviations covariance $\mathbf{C}_{elas}$,

$$\rho(\mathbf{m}_{elas} \mid \mathbf{m}_{res}, \mathbf{m}_{rmod}) = c\exp[-1/2\,(\mathbf{m}_{elas} - \mathbf{F}(\mathbf{m}_{res}, \mathbf{m}_{rmod})^T\,\mathbf{C}_{elas}^{-1}\,(\mathbf{m}_{elas} - \mathbf{F}(\mathbf{m}_{res}, \mathbf{m}_{rmod})]. \quad (5)$$

For the calibration of the rock-physics model, parameter initial priors were obtained by analysis of property crossplots derived from well logs. The well-log reservoir and elastic properties were upscaled appropriately to the seismic resolution for the calibration. Figure 3 shows histograms that describe the posterior frequencies of the rock-physics model parameters, obtained from the MCMC sampling chain.

A similar procedure was used for calibration of source wavelets. Initial priors were estimated by regular seismic-to-well-log tie. Then an MCMC sampling of the posterior density (equation 3) estimates the frequency of deviations of the source wavelets from the prior configuration to fit the seismic prestack gathers closest to well locations.

Seismic inversion for reservoir properties

The seismic AVA response of the gas-bearing sands in this field is characterized as class 2 AVA. Figure 4 depicts curves that show the modeled reflectivity at top and bottom of the reservoir for various saturations. These reflectivities were calculated with basis on the rock-physics model previously calibrated. The plot shows the dependency of the reflectivity on the saturation and incidence angle for two cases — a sequence of shale–gas sand–shale and a sequence of shale–gas sand–water sand.

In the seismic-inversion setting, common components of the posterior PDF are not the same as for the calibration steps. The prior information includes the calibrated estimates of the rock-physics model and the source wavelets. These variables are still random (nonconstant) at the inversion model but are subjected to smaller uncertainties than they were prior to calibration. On the other hand, for calibration of the rock-physics model parameters, the prior uncertainties about the reservoir properties were small because they corresponded to total porosity, shale fraction, and water saturation calculated from well logs. At the seismic-inversion step, because the objective is to estimate the reservoir parameters with nonlocalized well information, these prior uncertainties are large, and the central prior model for total porosity, shale fraction, and water saturation is poorly informative to avoid biasing the estimation.

We use a linear trend with the inversion window TWT for the total porosity and constant values for the shale fraction and water saturation. The linear trend of the porosity corresponds to the average linear trend observed in the well logs. The prior constant shale fraction corresponds to the average shale fraction in the inversion window for the wells, and the prior water saturation was taken close to one (no gas). The standard deviation from the prior central trends also was estimated from the well logs.

The MCMC sampling of the posterior PDF proceeds by first proposing candidates of the reservoir properties (porosity, shale fraction, and saturation) generated by multivariate

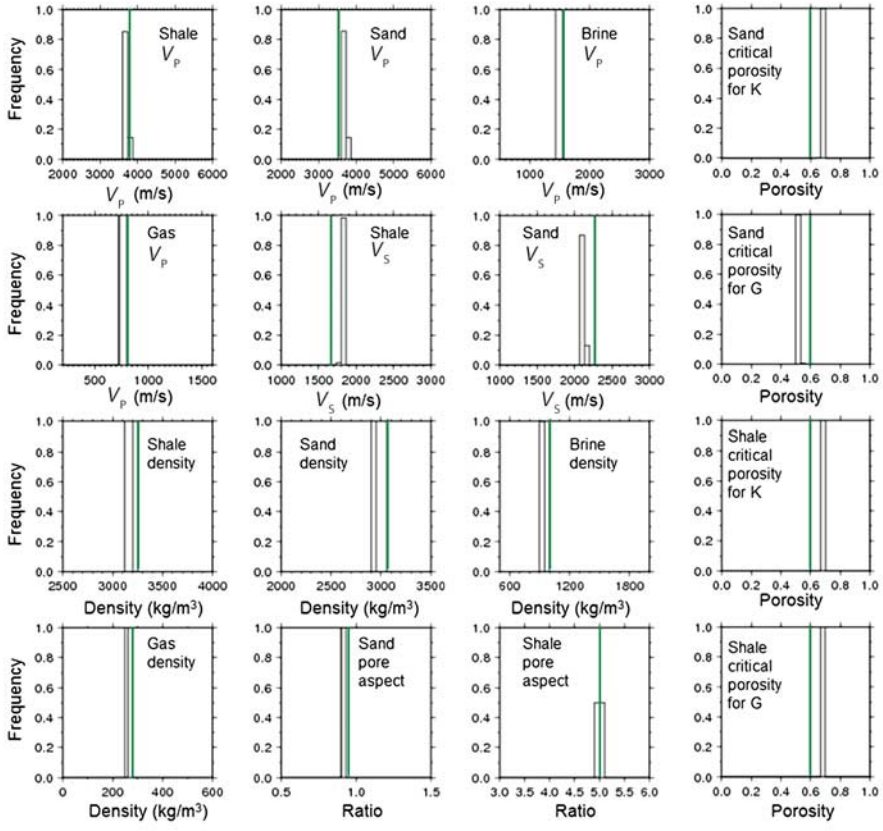

Figure 3. Posterior histograms for the rock-physics model calibration (black lines) and the prior value (green line) obtained by conventional crossplot analysis.

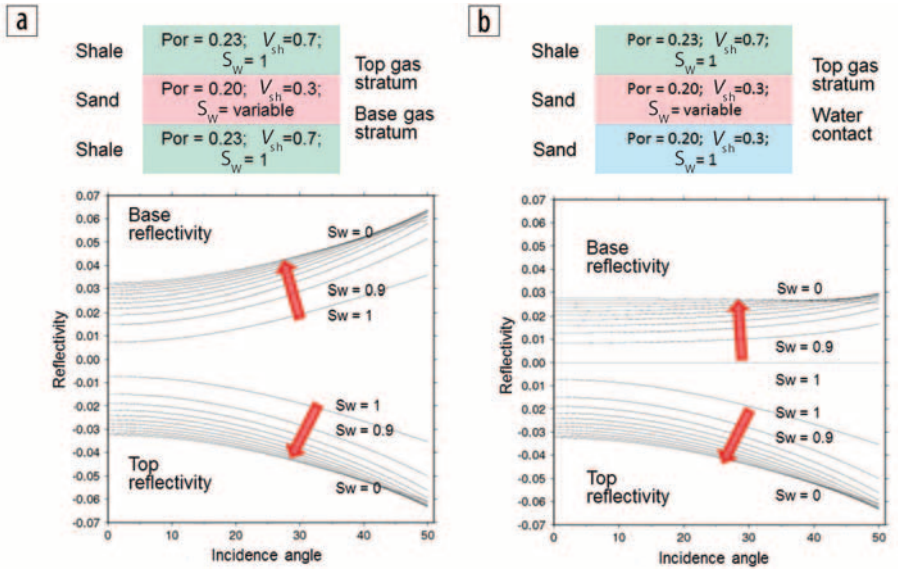

Figure 4. Reflectivity calculated at the top and bottom of the target sand as function of water saturation, S_w, and incidence angle for the scenarios of (a) shale seal, gas sand, and shale base and (b) shale seal, gas sand, and water contact.

Gaussian simulation of the prior PDF, $\rho(\mathbf{m}_{res})$. Second, a realization of the rock-physics model parameters is drawn from the prior PDF $\rho(\mathbf{m}_{rmod})$ with central values and deviations according to the results of the previous calibration against well data.

For the reservoir parameter configuration generated, the petrophysical transform is calculated for expected values of the elastic model parameters (V_P, V_S, and mass density). However, those values are not used directly for calculation of the seismic data because in this case, we would neglect the petrophysical transform uncertainty.

To produce the outcome of the elastic parameters according to the rock-physics conditional in equation 5, multivariate Gaussian deviates are produced according to the deviation covariance $\mathbf{C}_{elas}$ and are added to the central transform trend. These elastic-property parameters are used for calculation of reflectivities. In addition, a candidate source-wavelet deviation array is generated and is added to the prior central source wavelet to draw a source-wavelet outcome from the prior $\rho(\mathbf{m}_{source})$. The wavelets are convolved with the reflectivities according to the corresponding incidence angles to produce the calculated seismic gather. Finally, the likelihood function ratio between the candidate and the current configuration is evaluated, and the

Metropolis rule is applied to accept or reject the candidate joint model configuration. The procedure continues 50,000 times per CDP seismic gather.

To produce a new candidate configuration from the current one in the chain, the current configuration is perturbed locally in a given number of time zones located at random. In the perturbations, the vertical correlation and crosscorrelations among reservoir properties are accounted for through the multivariate simulation method used and the corresponding covariance functions modeled from the upscaled well-log data. The same methods are applied to produce the conditional realizations of the elastic-model parameters. The seismic-data misfit evaluation is given by the sum of squares of the amplitude residuals in the inversion time window for the full seismic gather.

Figures 5 and 6 describe the sampling results for the inversion of seismic gathers at four locations with available well information; two locations are shown in each figure, one with confirmed presence of gas and the other with absence of gas. Figures 5a and 6a show (magenta lines) plus and minus one standard deviation range from the trends that characterize the prior uncertainty used for the reservoir properties. The prior uncertainty on the water saturation was set with a Gaussian curve with maximum at the top of the target sand; the maximum gas saturation at one standard deviation was 0.5. This prior distribution of the saturation is the same for the gas-producing and nonproducing locations. Realizations of the MCMC at regular intervals in the chain are shown in green curves in these plots; a total of 10 realizations among 50,000 is plotted at the reservoir property domain (total porosity, shale fraction, and saturation) and at the elastic property domain (V_P, V_S, and mass density).

Figures 5c and 6c shows the corresponding observed seismic gathers at the incidence-angle domain. It is evident that the strong red-blue amplitude pair with class 2 AVA effect characterizes the two locations with gas, whereas the two dry locations do not show the characteristic seismic response. The calculated seismic gather corresponding to the average configuration sampled by the chain is shown to the left of the observed data. The frequency of realizations (among the 10 shown) that

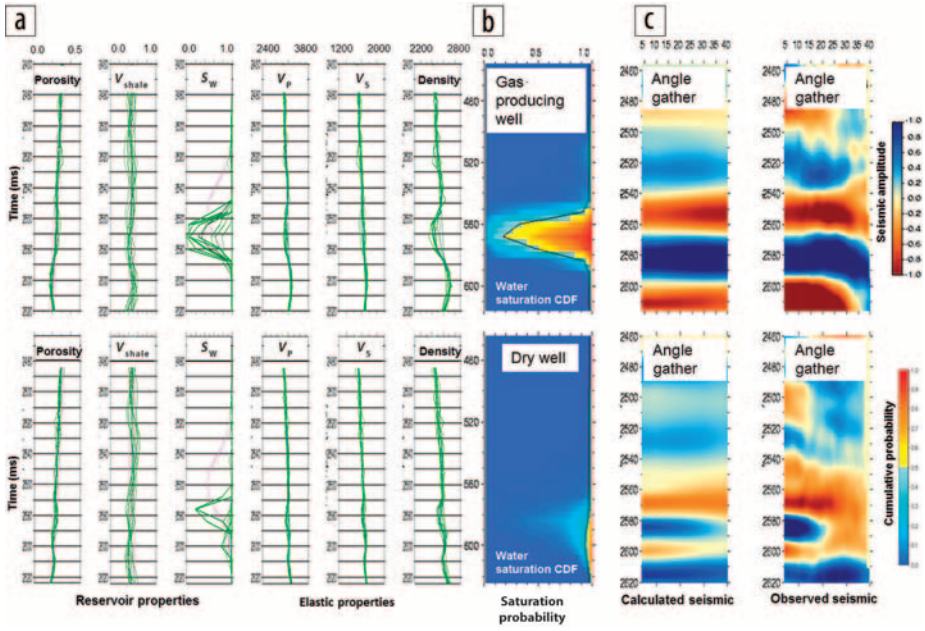

Figure 5. Ten realizations of the reservoir and elastic properties (green lines) drawn from the posterior PDF and the estimated marginal water saturation CDF calculated after 50,000 realizations for two CDP locations near a gas-producing well and a dry well. The seismic gather calculated from the estimated elastic configuration (average of the realizations) and the observed seismic gather are shown for each location. The magenta line marks plus and minus one standard deviation for the prior information of the water saturation, shale fraction, and total porosity. The black line shows the estimated profile for the elastic and reservoir properties.

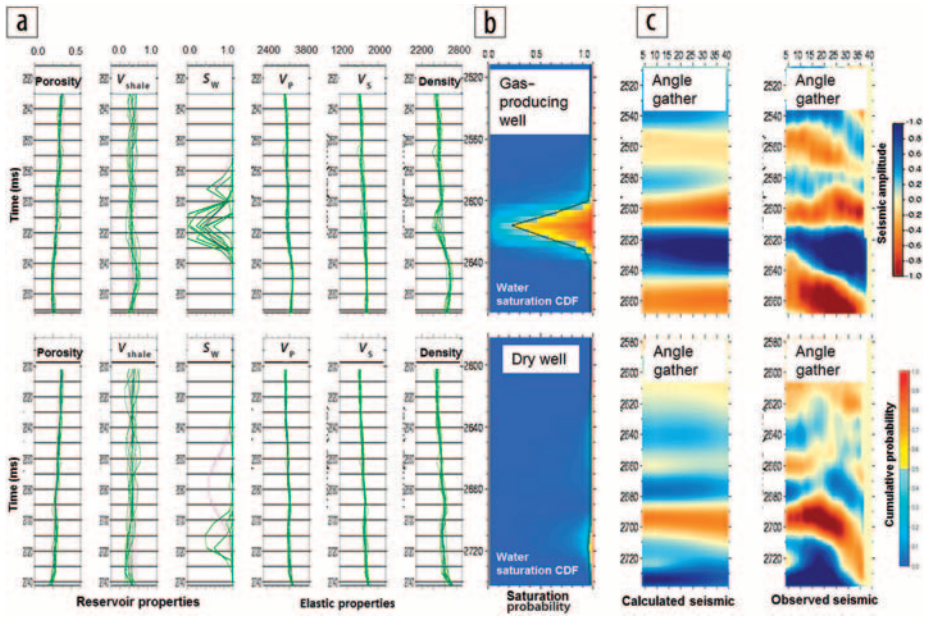

Figure 6. Ten realizations of the reservoir and elastic properties (green lines) drawn from the posterior PDF and the estimated marginal water saturation CDF calculated after 50,000 realizations for two CDP locations near a gas-producing well and a dry well. The seismic gather calculated from the estimated elastic configuration (average of the realizations) and the observed seismic gather are shown for each location. The magenta line marks plus and minus one standard deviation for the prior information of the water saturation, shale fraction, and total porosity. The black line shows the estimated profile for the elastic and reservoir properties.

exhibit gas saturation is large for the gas wells and small for the dry wells.

A summary of the information provided by the full sampling (the 50,000 realizations) is produced in the marginal cumulative distribution function histogram of the saturation shown in Figures 5b and 6b. The CDF accounts for the probability of the true water saturation to be smaller than the horizontal axis saturation and to increase monotonically from zero to one. The estimated saturation, which is the average of the saturation profiles at the sampling chain, is superposed in a black line in Figures 5b and 6b.

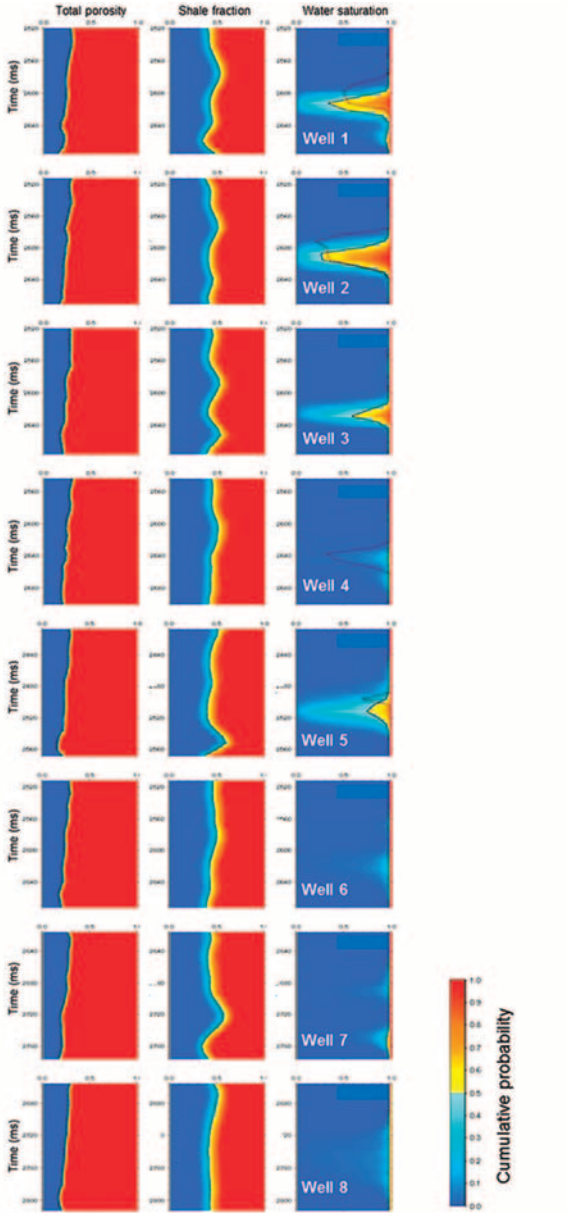

Figure 7. Cumulative probability distributions estimated by the seismic inversion for water saturation, shale fraction, and total porosity at locations close to eight control wells. The black line shows the estimated property value (average of the realizations), and the magenta line shows water saturation calculated from well logs.

The CDFs results show the probabilities for the gas saturation (complement of the water saturation) at the target sand, are positive for gas presence at the gas-producing wells, and indicate gas absence (or very low saturation) for the dry wells.

Figure 7 shows the results at the locations corresponding to the eight control wells used, with indications of the saturation evaluated from the well logs. Saturation from the well logs shows a good match with the estimated saturation by the MCMC sampling for almost all wells. Well 3 had no well-derived saturation because of absence of one of the logs, but it is a gas-producing well. Well 4 is a gas producer with good gas saturation and does not comply with the prediction by the method as a dry well. However, this well is at the border of the gas compartment, and the seismic gas signature is not present in the data.

Description of the probability distributions was exploited further to calculate probability in derived parameters such as the expected in situ gas volume at an expected gas compartment or expected sand-gas thickness displayed in maps.

Conclusions

The formulation of a combined rock-physics and seismic inverse problem is useful in mapping the uncertainties associated with various steps of modeling and observation involved in the inference of reservoir parameters such as saturation, porosity, and shale fraction. Probabilistic formulation of this problem and its solution using Markov-chain Monte Carlo methods provides a description of the uncertainties via marginal cumulative distribution functions or cumulative probability densities for the reservoir parameters. An example of a gas reservoir with Class 2 AVA response showed coherency of the estimated CDF with the known saturation at various well locations. An important issue for reliability of the combined model is related to calibration of its components (rock physics and seismic) for the specific target, under the assumption of spatial homogeneity of the seismic and reservoir characterization — prior reservoir statistics, calibrated rock-physics model, prior source-wavelet statistics, seismic amplitude, and migration accuracy. TLE

Acknowledgments

We thank Pacific Rubiales Energy and Info Geosciences Technology and Services for their authorization to publish the information shown in this article.

Corresponding author: boschme@gmail.com

References

Bosch, M., T. Mukerji, and E. Gonzalez, 2010, Seismic inversion for reservoir properties combining statistical rock physics and geostatistics: Reviews of Geophysics, **75**, A165–A176, http://dx.doi.org/10.1190/1.3478209.

Grana, D., M. Pirrone, and T. Mukerji, 2012, Quantitative log interpretation and uncertainty propagation of petrophysical properties and facies classification from rock-physics modeling and formation evaluation analysis: Geophysics, **77**, no. 3, WA45–WA63, http://dx.doi.org/10.1190/geo2011-0272.1.